

## Three-Dimensional Design of Axial Flow Compressor Blades Using the Ball-Spine Algorithm

A. Madadi<sup>1</sup>, M.J. Kermani<sup>1†</sup> and M. Nili<sup>2</sup>

<sup>1</sup> *Department of Mechanical Engineering, Amirkabir University of Technology (Tehran Polytechnic), Tehran, Iran, P. Code 15875-4413*

<sup>2</sup> *Department of Mechanical Engineering, Isfahan University of Technology, Isfahan, Iran*

† *Corresponding Author Email: mkermani@aut.ac.ir*

(Received September 24, 2013; accepted August 13, 2014)

### ABSTRACT

Recently a new inverse design algorithm has been developed for the design of ducts, called ball-spine (BS). In the BS algorithm, the duct walls are considered as a set of virtual balls that can freely move along some specified directions, called ‘spines’. Initial geometry is guessed and the flow field is analyzed by a flow solver. Comparing the computed pressure distribution (CPD) with the target pressure distribution (TPD), new balls positions for the modified geometry are determined. This procedure is repeated until the target pressure is achieved. In the present work, the ball-spine algorithm is applied to three-dimensional design of axial compressor blades. The design procedure is tested on blades based on NACA65-410 and NACA65-610 profiles and the accuracy of the method is shown to be very good. As an application, the pressure distribution of the blade with NACA65-610 profiles is modified and the pressure gradient in the aft part of the blade is decreased and selected as target pressure distribution. The corresponding geometry which satisfies the target pressure is determined using the BS design algorithm.

**Keywords:** Ball-Spine algorithm; Inverse design; Compressor blade; Target pressure distribution.

### NOMENCLATURE

$A$	element area [m <sup>2</sup> ]	$P_0$	total pressure [Pa]
$a$	acceleration of the ball [m/s <sup>2</sup> ]	$TPD$	target Pressure Distribution [Pa]
$C$	geometry correction coefficient [m <sup>2</sup> s <sup>2</sup> /kg]	$x$	x position of the ball [m], x coordinate
$CPD$	computed Pressure Distribution [Pa]	$y$	y position of the ball [m], y coordinate
$d$	distance of the ball from chord line [m]	$\Delta P$	pressure difference [Pa]
$Error P$	pressure error parameter	$\Delta PD$	distribution of pressure difference [Pa]
$Error S$	displacement error parameter	$\Delta s$	displacement of the ball [m]
$F$	force imposed on the ball [N]	$\Delta t$	time step[s]
$i$	node index from leading to trailing edge		
$j$	node index from hub to tip	<b>Subscripts</b>	
$J_{max}$	no. of nodes from hub to tip	Comp.	computed conditions
$L_c$	blade chord length [m]	LE	leading edge
$m$	ball mass [kg]	new	new conditions
$n_x$	x-component of normal vector	old	old conditions
$n_y$	y-component of normal vector	Target	target conditions
$P$	static pressure [Pa]	TE	trailing edge

### 1. INTRODUCTION

Design of hardware involving fluid flow or heat transfer such as intakes, manifolds, compressor and turbine blades, etc., is defined as the shape determination of the solid elements so that the flow or heat transfer rate is optimized in some sense.

Often, both Computational Fluid Dynamics (CFD) and design algorithms are involved in determining the optimal shape. The computational costs in design techniques are usually a challenge, so an appropriate algorithm for the rapid shape determination is always of interest to designers.

In general, the design problems are categorized in two

groups, optimization problems and inverse design problems. In the first group, an objective function, which can be compounded of various targets, is defined and using optimization algorithms, the optimum values for the design parameters of the function are determined. Li *et al.* (2006) developed a blading design optimization system using an aeromechanical approach and harmonic perturbation method. They implemented this method on NASA 67 rotor and improved the efficiency of the rotor by 0.4% considering the stress limitations. Verstraete *et al.* (2007) presented a multidisciplinary optimization and applied it to the design of a small radial compressor impeller. In this method a genetic algorithm and artificial neural network have been used to find geometry with maximum efficiency regarding a maximum stress limitation in the blades.

For the second type of design problems, i.e. inverse design ones, there are basically two different algorithms to solve the design problems: decoupled (iterative) and coupled (direct or non-iterative) techniques. In the coupled solution approach an alternative formulation of the problem is used in which the surface coordinates appear (explicitly or implicitly) as dependent variables. In other words, the coupled methods tend to find the unknown part of the boundary values and the flow field unknowns simultaneously in a (theoretically) single-pass or one-shot approach. More information can be found in Lamm (1993). Equations of coupled methods make the set of the governing equations very complicated; hence these methods are limited to simple flow regimes.

On the other hand, the iterative design approach solves a series of sequential problems in which the geometry is modified in each step (evolved) so that the desired TPD is eventually achieved (See Garabedian and McFadden 1982). In these iterative methods, the governing equations are similar to the flow field equations and the conventional solvers could be used as a black box. Hence the iterative methods are applicable for complicated flow regimes.

The traditional iterative methods used for inverse design problems are often based on trial and error or optimization-search algorithms. The trial and error search process is very time-consuming and computationally expensive; it also depends on the designer's experience.

The iterative methods presented so far use the physical algorithms instead of the mathematical ones to automate the geometry modification in each iteration cycle. The physical-based methods are easier and quicker than the mathematical (or optimization based) iterative schemes. Nili-Ahmadabadi *et al.* (2009) presented an iterative inverse design method for internal flows called Flexible String Algorithm (FSA). They considered the duct wall as a flexible string frequently deformed under the difference between TPD and CPD,  $\Delta PD = TPD - CPD$ . They developed this method for non-viscous compressible (Nili-Ahmadabadi 2010 a) and viscous incompressible internal flow regimes (Nili-Ahmadabadi 2010b). Recently, Nili *et al.* (2010c), have presented a novel inverse design method called Ball-Spine algorithm (BS algorithm). They developed this method for quasi-3D

design of meridional plane of centrifugal compressors (Nili *et al.* 2013). In a recent paper, Madadi *et al.* (2011) applied the ball-spine algorithm to 2D design of sharp leading edge airfoils.

In this paper, the method is applied to three-dimensional design of axial flow compressor blades. To do so, the ball spine algorithm is applied section by section from hub to tip of compressor blade. The method is applied to three test cases in this paper. Two compressor blades based on NACA65-410 and NACA65-610 profiles are selected as validating cases and a new blade with a modified pressure gradient of NACA65-610 blade is designed as an application of the method.

It should be noted that the performance of an axial compressor depends on all stages, rotors, stators, chord length, tip clearance and numerous other parameters. In this paper, the authors focused on the design of the blade profiles which are used in the detail design step of an axial compressor design procedure. In practice, after preliminary design of an axial compressor, main parameters such as number of blades, chord length, hub-tip ratio, camber angle, lift coefficient, etc. are obtained. In the detail design step, the designer can use the ball spine method to design a blade which satisfies the given lift coefficient.

The main advantage of this method is that in the ball spine algorithm, a relation between a physical quantity which is pressure and the geometry is introduced. Hence, the convergence rate of this method is very faster than other design techniques such as optimization based methods. On the other hand, the designer can use this method to improve the blade performance by diminish the separation regions regard to a convenient pressure distribution. For example if a separation zone is presented in the domain, the designer can use a pressure distribution with lower adverse pressure gradient to prevent the flow separation. Now, using the ball spine algorithm, the corresponding blade profile can be obtained.

## 2. FLOW FIELD SOLUTION

To solve the inviscid flow field within the three-dimensional domain, a recently developed in-house code based on the flux difference splitting (FDS) scheme of Roe (1981) is used. The governing equations are discretized using the formulations presented by Kermani (2001).

The Roe scheme gives non-physical expansion shocks in the regions where the eigenvalues of the Jacobian matrix vanish, e.g., the sonic regions and stagnation points. To solve this problem, an entropy correction formula from Kermani and Plett (2001) is used here. Grids are generated using an in-house code based on algebraic and elliptic grid generation methods.

## 3. THE BALL-SPINE (BS) ALGORITHM

In the present work, the ball-spine algorithm is

applied to three-dimensional design of a compressor blade. For better understanding, at first the basis of the ball spine algorithm is explained for a two-dimensional duct. Then the method is explained for three-dimensional geometries.

Here, the duct wall is considered as a set of virtual balls allowed to be freely moved along the specified direction called spines, shown in fig.1 Passing fluid flow through the flexible duct causes a pressure distribution to be applied to the outer side of the wall. If a target pressure distribution is applied to the inner side of the wall on each ball, the flexible wall deforms to reach a shape satisfying the target pressure distribution. In other words, the force due to the difference between the target and computed pressure distribution at each point on the wall is applied to each virtual ball and causes them to move. As the target shape is obtained, this pressure difference vanishes and the balls will stop moving.

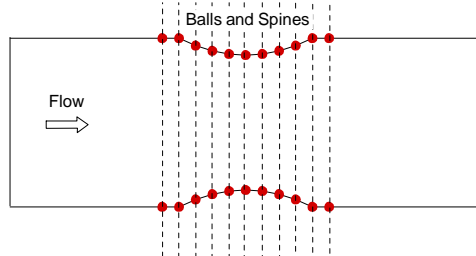


**Fig. 1. 2-D duct with balls and spines.**

To derive the kinematic relations of a flexible wall, a uniform mass distribution along the wall is supposed. Now a sample ball on the duct wall is considered. The net force applied to the ball along the spine direction is computed as,

$$F = \Delta P \cdot A \quad (1)$$

where,

$$\Delta P = P_{Target} - P_{Comp.} \quad (2)$$

and  $A$  is the area of each element (or projected area of the ball). If a ball moves along the spine through a specified time step ( $\Delta t$ ), the corresponding displacement is computed from the following dynamic relations,

$$\Delta s = \frac{1}{2} a (\Delta t)^2, \quad a = \frac{F}{m} \quad (3)$$

where,  $m$  and  $\Delta s$  are the mass and displacement of the ball, respectively. Substituting Eqs. (1) and (2) into Eq. (3) yields,

$$\Delta s = \frac{1}{2} \frac{A}{m} (\Delta t)^2 (P_{Target} - P_{Comp.}) \quad (4)$$

or,

$$\Delta s = C \cdot \Delta P, \quad \Delta P = (P_{Target} - P_{Comp.}) \quad (5)$$

where,  $C = A(\Delta t)^2 / 2m$  which is called ‘‘Geometry Correction Coefficient’’ has the dimensions of  $[m^2 \cdot s^2 / kg]$ . Using the computed displacement for each ball (or computational node) on the wall, new geometry is obtained. Grids are generated for new geometry and the flow field is solved using flow solver. The procedure is repeated until the target and computed pressure distributions met and the

balls positions become fixed. The design algorithm is shown in fig. 2

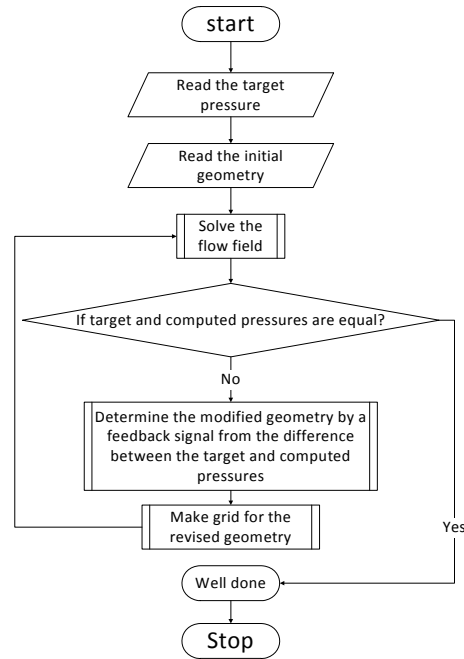


**Fig. 2. Design flowchart.**

Now the method is explained for a two-dimensional compressor airfoil. For this case, the flow field is solved within a two-dimensional compressor cascade which is shown in fig. 3 The balls on the blade surfaces, the spine directions, and the boundary conditions are also presented.

The direction normal to the chord line is selected as the spine for the airfoils shown in fig. 4 As shown in 0fig. 3, in the present work the compressor cascade is considered as a duct but to give a better sense to the reader, using a translational mapping by cascade pitch, the airfoil geometry is shown in fig. 4.

The new position of each ball is calculated as follows:

$$y_{new} = y_{old} + \Delta s \cdot n_y \quad (6)$$

and,

$$x_{new} = x_{old} + \Delta s \cdot n_x \quad (7)$$

where,  $n_x$  and  $n_y$  are the components of the spine direction vector normal to the blade chord line shown in fig. 4.

Because the wall is considered as a set of separated balls, during the design process, the wall curvature may be discontinuous in adjacent nodes (balls). An example of such discontinuity is shown in fig. 5. To smooth the wall curvature, a filtration scheme is applied to the ball distance from the chord line after each geometry correction step. The filtration scheme is formulated as follows,

$$d_i = \frac{d_{i-1} + 2d_i + d_{i+1}}{4} \quad (8)$$

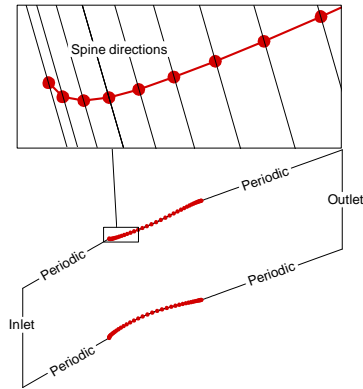


**Fig. 3. Computational domain for compressor cascade, balls and spine directions.**

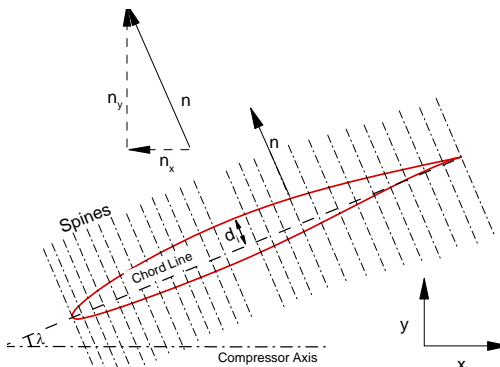


**Fig. 4. Spine directions for design of airfoils.**

where  $d_i$  is the distance of the  $i$ -th ball from the blade chord line (see 0fig. 4). In 0fig. 5, the filtered geometry is plotted using a dashed line.

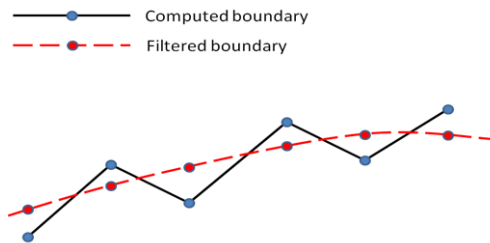


**Fig. 5. Wall boundary filtration.**

For compressor blade design, a target pressure distribution is given for each airfoil surface i.e. suction side and pressure side. To satisfy both distributions, the geometry correction is done on both surfaces. Finally, when both pressure distributions match, the geometry is fixed.

The method is explained for tow-dimensional design of a compressor blade cascade. Now, to extend the method to three-dimensional design of a compressor blade profile, several sections are selected from hub to tip of the compressor blade shown in fig. 2 The inverse design method explained before is used to design of each section. It means that the-three dimensional target pressure distribution is considered on the blade surfaces. The three-dimensional flow field is solved in the blade passage and the pressure distribution on the blade surface at each section is computed. In the geometry correction step, the ball movements are done

at each section marching from hub to tip of the blade. The designer can select the number of sections from hub to tip of the blade. In the present work, the sections are selected on each grid layer from first which is at the hub to the last which is at the tip of the blade. It should be noted that the flow field solution is done using 3D flow solver and the 3D effects are considered here. To make better comparison, results are shown for hub and tip sections.

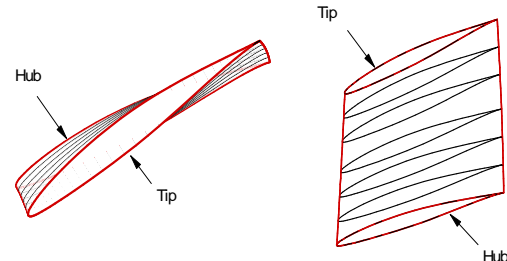


**Fig. 6. Sections from hub to tip of the blade used for three-dimensional design of blade profile.**

In Eq. (5) a parameter  $C$  is introduced as Geometry Correction Coefficient. Considering a large value for the parameter  $C$  causes the balls displacements to increase and the convergence rate to be improved. On the other hand, if the parameter  $C$  exceeds a limit, the solution becomes unstable. Although a small value of  $C$  causes the design procedure to be stable, the convergence rate decreases. Hence, an optimum value for the geometry correction factor should be determined. In the present work, the balls are supposed on each computational node on the wall. This selection makes the implementation of the method easier. Someone can use different number of balls and uses an interpolation method to compute the intermediate node displacements.

Here, the inviscid flow solver is used to improve the speed of the method. Also the viscous solver could be used as flow solver. It is an advantage of the ball spine method that the flow solver is used as a black box and the designer can use any in-house flow solver and commercial ones. Because the method is used the pressure distribution for geometry correction and while no separation region exists, the trend of pressure distribution for inviscid and viscous flows over a body are similar, the designer can use an inviscid flow solver to have a faster design code. Of course, using a viscous flow solver can improve the accuracy of the method. As an alternative, the designer can study the viscous flow through the domain after the design procedure to evaluate the performance of the method. If needed, the designer can modify the target pressure distribution regarding to fluid dynamics and boundary layer concepts and use a more convenient pressure distribution (for example a pressure distribution with lower adverse pressure gradient) and repeat the design procedure to achieve an acceptable performance.

#### 4. RESULTS AND DISCUSSION

In the present work, the ball-spine method is applied to three-dimensional design of compressor blade profiles and evaluated for three test cases. At first, as a validation test case, a compressor blade based on

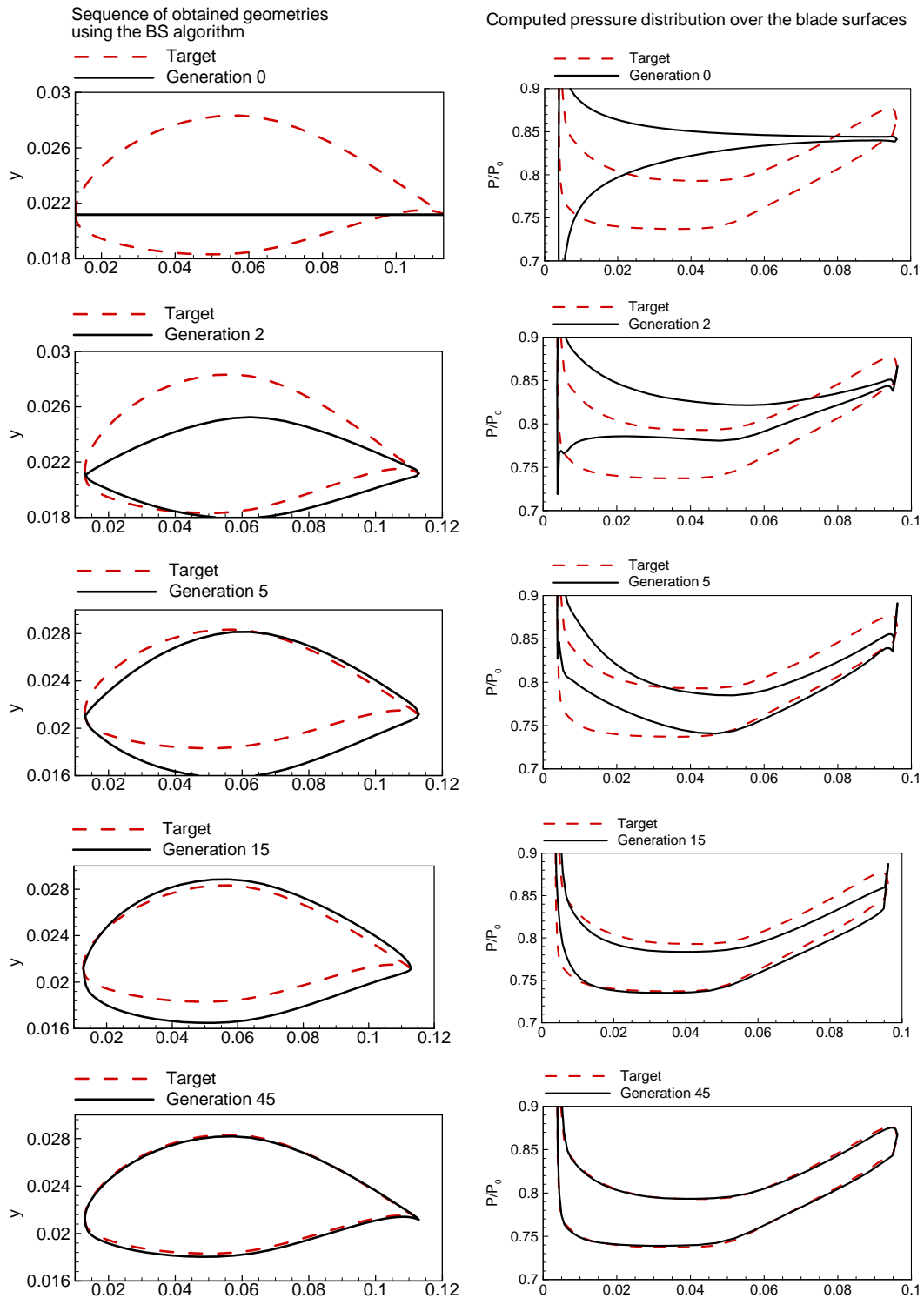


**Fig. 7. Evolution of geometries and their corresponding pressure distributions from the initial guess (Generation 0) toward the target geometry; hub section.**

NACA65-410 profiles is considered. The blade is composed of NACA65-410 profile which has a stagger angle of 22.50 at the hub section and a stagger angle of 32.50 at the tip section. At first the flow field within the domain of the target geometry is solved and the obtained pressure distribution from the hub section to the tip section is considered as the target pressure distribution. The initial guessed geometry is selected as a blade composed of flat plate airfoils

from hub to tip with stagger angle similar to the target geometry. Now the design procedure is started from mentioned initial guessed geometry and using the considered target pressure distribution the design process is continued to reach the target pressure distribution.

In fig. 7, the design history is shown by geometry generations and corresponding pressure

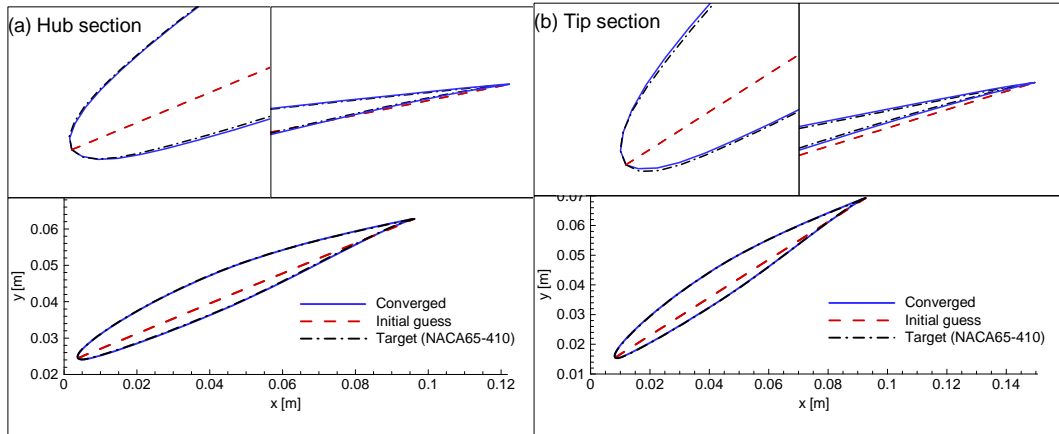


**Fig. 8. Initial guess, target and converged geometries for NACA65-410 test case; (a) hub section, (b) tip section.**

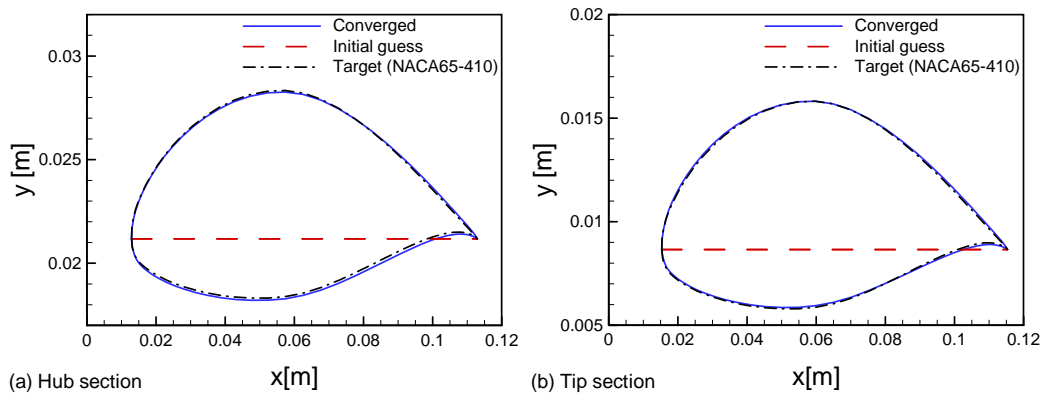


**Fig. 9. Blade profiles for NACA65-410 test case, magnified in y-direction; (a) hub section, (b) tip section.**

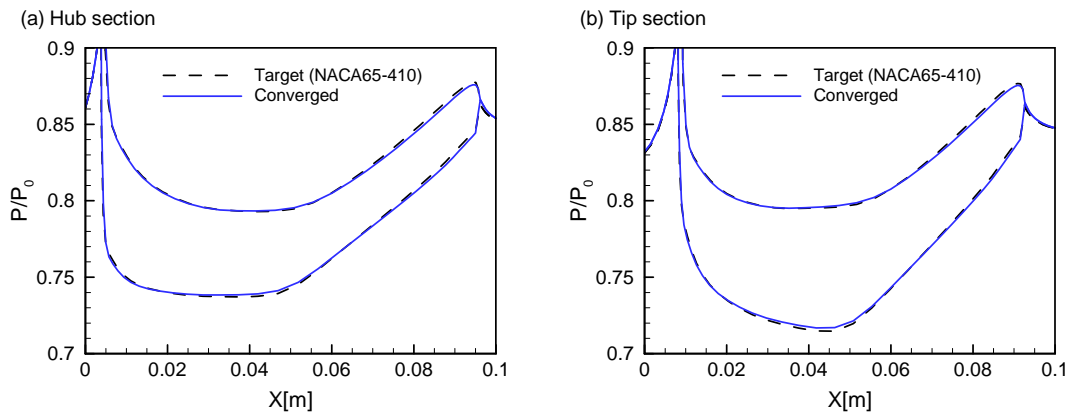


**Fig. 10. Target and converged pressure distributions for NACA65-410 test case; (a) hub section, (b) tip section.**

distributions at hub section. As it is seen, after 45th generation the target and computed pressure distributions match and the shape modification is stopped. It is reminded again that the compressor blade passage is considered as a three-dimensional duct (a two-dimensional section is shown in fig. 3), and to have a better view of the blade, using a translation by cascade pitch the blade geometry is presented in the following figures of the paper.

In fig. 8, the initial and target geometries with the

final converged one are illustrated and compared at hub and tip sections. As shown, a view point near the leading and trailing edges is magnified for better comparison. According to this figure, the final converged geometry is very close to the target geometry. In 0fig. 9, the blade profiles at hub and tip sections are presented and magnified in y-direction. The convergence of the method is emphasized in this figure.

In fig. 10, the converged pressure distribution is

compared with the target pressure distribution at hub and tip section; the results indicate a good agreement. In Fig. 11, the convergence history is shown by pressure and displacement error parameter defined as,

$$Error P = \frac{\sum_{j=1}^{J_{max}} \sum_{i=i_{LE}}^{i_{TE}} |(P_{Target} - P_{Comp.})_i|_{Blade\ surface}}{J_{max} \times (i_{TE} - i_{LE} + 1) \times P_0} \quad (9)$$

$$Error S = \frac{\sum_{j=1}^{J_{max}} \sum_{i=i_{LE}}^{i_{TE}} |\Delta S|_{Blade\ surfaces}}{J_{max} \times (i_{TE} - i_{LE} + 1) \times L_C} \quad (10)$$

where  $P_0$  is the total pressure,  $\Delta S$  is the displacement of each ball and  $L_C$  is the blade chord length. The design process converges after about 40 geometry modifications.

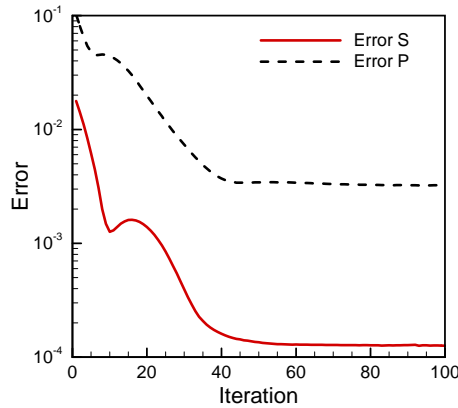


**Fig. 11. Convergence history for NACA65-410 test case, Error P and Error S are introduced in Eqs. (9) and (10).**

In fig. 12, the convergence history of the design process is shown for different values of geometry correction coefficient  $C$ . The convergence rate is increased as the coefficient  $C$  is increased to an optimum value of  $50 \times 10^{-9}$ . More increase in values of  $C$  results in divergence of the method. It is concluded that for a design process an optimum or critical value of geometry correction coefficient,  $C$ , should be determined.

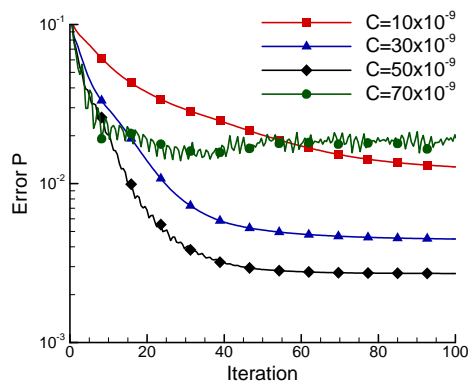


**Fig. 12. Effect of geometry correction coefficient, C, on convergence rate of the design process.**

For the second validation test case, the approach is applied to a blade composed of NACA65-610 airfoil having a greater lift coefficient than NACA65-410 airfoil. In this case, the NACA65-410 blade (previous test case) is considered as the initial guessed geometry and the pressure distribution of NACA65-610 blade is considered as the target one. In Fig. 13, the initial, target and converged geometries are illustrated and magnified in y-direction at hub and tip sections. The comparison between the converged and target geometries shows a good agreement. Moreover, the comparison between the initial, target and converged pressure distributions at hub and tip section is presented in fig. 14. It is clear that the converged and target pressure distributions coincide.

The previous test cases were studied for validation of the ball-spine algorithm. Here, as an applied example, a new target pressure distribution is considered and the accuracy and applicability of the method is assessed. To do so, the pressure distribution of NACA65-610 blade is considered and the location of minimum pressure is moved toward the blade leading edge. This change decreases the adverse pressure gradient on the aft part of the blade. For this test case, starting from NACA65-610 blade as the initial guessed geometry, the design process converges to the corresponding blade. In Fig. 15, the target, the initial (corresponds to NACA65-610 blade) and the converged pressure distributions are compared at hub and tip sections. As it is seen, the location of minimum pressure is moved toward the blade leading edge. The converged and target pressures have acceptable agreement.

In Fig. 16, the initial guessed geometry (NACA65-610 blade) and the new designed blade at hub and tip sections are compared.

## 5. CONCLUSIONS

Recently a Ball –Spine (BS) algorithm has been proposed and its accuracy has been assessed for tow-dimensional geometries. In this paper, the method is extended to the design of three-dimensional compressor blades. To do so, the ball spine algorithm is applied section by section from the hub to the tip of the blade. During the design process, the flow field is solved using a 3D solver and 3D effects are considered. The method was applied to two blades based on NACA65-410 and NACA65-610 profiles as validating test cases and the results show good agreements with the target pressures and geometries. Then as an extension, based on the pressure loadings of NACA65-610 a new target pressure was introduced to decrease the adverse pressure gradient in the aft part of the blade. The design algorithm was applied and the geometry of the new designed airfoil was obtained, which matches the considered target pressure very well. In the present work, the method is developed for subsonic airfoils. As an extension, the method could be implemented for transonic and supersonic conditions.

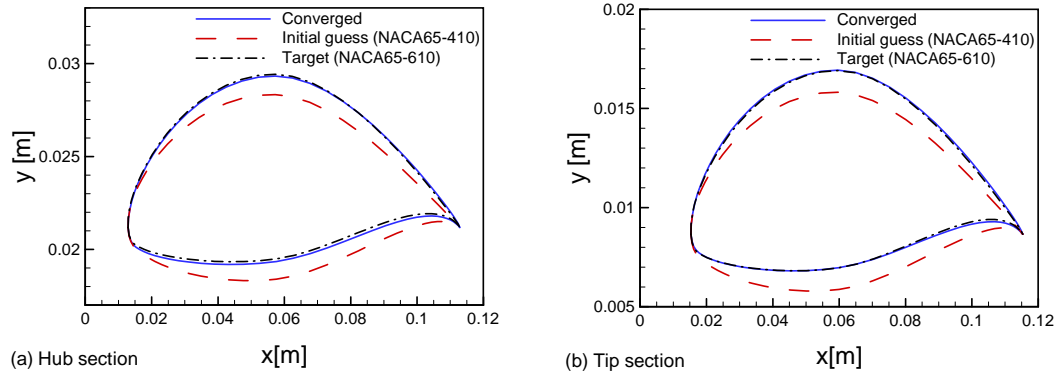


**Fig. 13. Blade profiles for NACA65-610 test case, magnified in y-direction; (a) hub section, (b) tip section.**

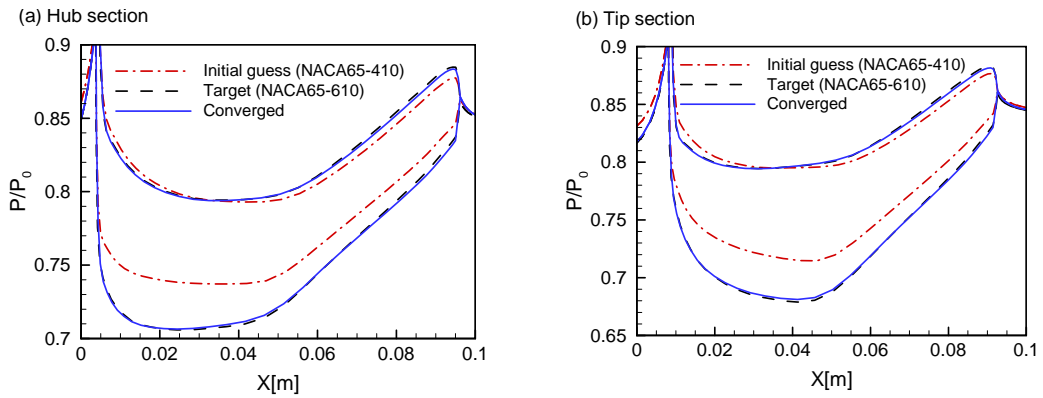


**Fig. 14. Comparison of initial, target and converged pressure distributions for NACA 65-610 test case; (a) hub section, (b) tip section.**

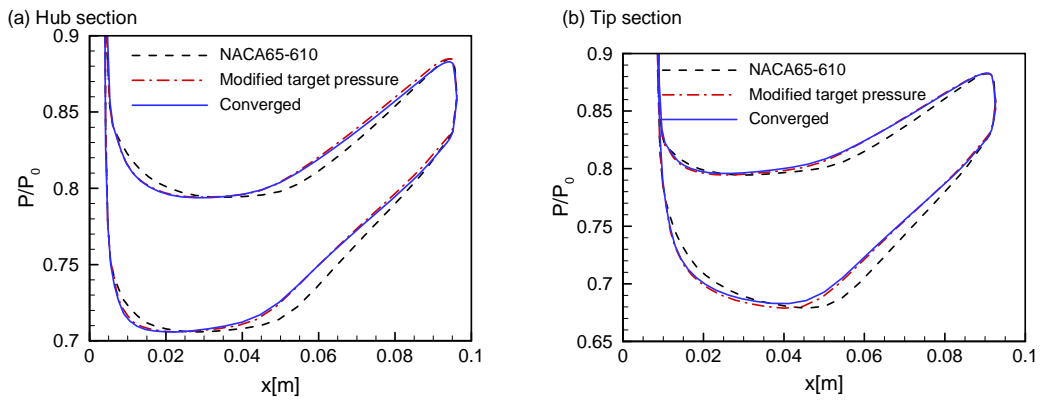


**Fig. 15. Comparison of initial pressure, modified target pressure and new designed airfoil pressure distributions; (a) hub section, (b) tip section.**

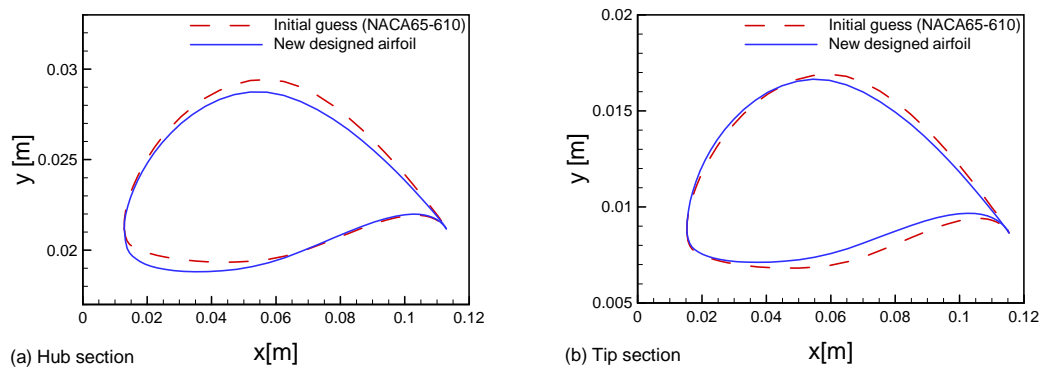


**Fig. 16. Blade profiles for new designed airfoil, magnified in y-direction; (a) hub section, (b) tip section.**

## REFERENCES

- Garabedian, P. and G. McFadden (1982). Design of supercritical swept wings. *AIAA Journal*. 30(3).
- Kermani, M. J. (2001). Development and Assessment of Upwind Schemes with Application to Inviscid and Viscous Flows on Structured Meshes. Ph.D. Thesis, *Department of Mechanical & Aerospace Engineering*, Carleton University, Canada.
- Kermani, M. J and E. G. Plett (2001). Modified Entropy Correction Formula for the Roe Scheme. *AIAA* 2001-0083.
- Lamm, P. K. (1993). Inverse Problems and Ill-Posedness. *Inverse Problems in Engineering: Theory and Practice*, ASME.
- Li, H. D., L. HeY., S. Li and R. G. Wells (2006). Blading Aerodynamics Design Optimization with Mechanical and Aeromechanical Constraints. *Proceedings of ASME Turbo Expo*, Barcelona, Spain, GT2006-90503.
- Madadi, A., M. J. Kermani and M. Nili-Ahmadabadi (2011). Application of an Inverse Design Method to Meet a Target Pressure in Axial-Flow Compressors. *Proceedings of ASME Turbo Expo*, Vancouver, Canada, GT2011-46091.
- Nili-Ahmadabadi, M., M. Durali, A. Hajilouy and F. Ghadak (2009). Inverse Design of 2D Subsonic Ducts Using Flexible String Algorithm. *Inverse Problems in Science and Engineering* 17(8),1037-1057.
- Nili-Ahmadabadi, M., A. Hajilouy, M. Durali and F. Ghadak (2010). Duct Design in Subsonic and Supersonic Flow Regimes with and without Normal Shock Waves Using Flexible String Algorithm. *Scientia Iranica Journal* 17(3),179-193.
- Nili-Ahmadabadi, M., A., F. HajilouyGhadak and M. Durali (2010). A Novel 2-D Incompressible Viscous Inverse Design Method for Internal Flows Using Flexible String Algorithm. *Journal of Fluids Engineering*, ASME., 132/031401-1-9.
- Nili-Ahmadabadi, M., M. Durali and A. Hajilouy (2010). A Novel Quasi-3D Design Method for Centrifugal Compressor Meridional Plane. *Proceedings of ASME Turbo Expo*, Glasgow, UK, GT2010-23341.
- Nili-Ahmadabadi, M., M. Durali and A. Hajilouy (2013). A Novel Aerodynamic Design Method for Centrifugal Compressor Impeller. *Journal of Applied Fluid Mechanics* 7(2), 329-344.
- Roe, P. L. (1981). Approximate Riemann Solvers, Parameter Vectors and Difference Schemes. *Journal of Computational Physics* 43,357-372,
- Verstraete, T., Z. Alsalihi and R. A. Van den Braembussche (2007). Multidisciplinary Optimization of a Radial Turbine for Micro Gas Turbine Applications. *Proceedings of ASME Turbo Expo*, Montreal, Canada, GT2007-27484.